Electric-field-modified heat capacity of adsorbed dipolar molecules

Ying-Yen Liao*

Department of Applied Physics, National University of Kaohsiung, Kaohsiung 811, Taiwan

The heat capacity of an adsorbed-molecule system is systematically investigated in electric fields. The energy spectrum is evaluated to probe the hindered rotation of the molecule. Numerical results demonstrate that the electric field and quantum confinement effect strongly affect the rotational characteristics of the molecule. The remarkable energy spectrum dominates the feature of heat capacity. Specifically, the heat capacity displays two explicit peaks, resulting from the anticrossing in the ground state. The effect of temperature on the peaks is further analyzed. In addition, the heat capacity shows a transferred behavior, depending on structural parameters.

I. INTRODUCTION

The properties of molecular rotation have attracted considerable research interest in chemistry and physics, ranging from chemical reaction to quantum-information processing.[1–3] The molecule has the superiority of controllability via external influences. For static electric field, the rotational energy levels of a free molecule are split due to the interaction between molecular dipole moment and electric field.[4] When the electric field becomes strong, molecular rotational-state energies conduct large negative shifts.[5] Moreover, the electric field diversifying with time, such as laser, can generate a superposition of rotational states. The phenomenon allows one to manipulate the spatial direction of molecules (i.e., molecular alignment and orientation).[6,7] Accordingly, understanding and controlling rotational behavior which exists through external influences is extremely important in the molecule-based systems.[8–10]

When a molecule is adsorbed or trapped on a solid surface, the rotational motion of the molecule is hindered and distinguished from that of a free rotor.[11,12] The rotational properties are strongly affected by the interaction between the molecule and its surrounding environment. Several experiments, such as electron energy loss spectroscopy, neutron scattering, and laser-induced desorption, are performed to probe the rotational properties of adsorbed molecules.[13–15] Simultaneously, theoretical research is devoted to single and more complex rotor systems that are subject to a different confining potential.[16–19] However, the research of exploring the external influence on hindered rotation is still minor, especially for thermodynamics. To exploit the field, we aim to investigate the effect of the hindered rotation on thermodynamic properties of adsorbed molecules under the electric field. It is extensively accepted that the thermodynamic properties depend on the energy dispersion of the system. The electric field enables one to modify the energy structure of the rotational states of the molecules.[20,21] Therefore, these modifications in energy structure are anticipated to reveal some interesting properties.

In the research, we study the heat capacity of adsorbed-molecule system in the presence of static electric field. After using exact diagonalization, numerical results show that the electric field effectively modifies the rotational characteristics of the molecules. The altered energy levels reveal the anticrossing behavior. In particular, the low-temperature heat capacity clearly indicates the remarkable feature due to the particular energy structure. The heat capacity shows two peaks near the anticrossing in the ground state. Furthermore, the structure and temperature parameters actually influence the behavior of heat capacity.

II. MODEL AND METHOD

The study considers a polar diatomic molecule is firmly adsorbed on a surface. The adsorbed molecule is subject to the surface potential. As illustrated in Fig. 1, the conical well is proposed to model the surface potential. For the structure of the well, the dependence on θ is stronger than that on ϕ.[16,17] To simplify the model, the well is assumed to be independent of ϕ. As a result, the well is partitioned into two regions with different potential barriers. The molecule motion is restricted in such a configuration. In addition, a static electric field parallel to the z axis is externally applied to modify the rotational properties of the molecule. Within the rigid-rotor approximation, the total Hamiltonian is expressed as

$$H = B\mathbf{J}^2 + V_{\text{hin}} + V_{\text{ext}}, \tag{1}$$

where B is the rotational constant, $\mathbf{J}$ is the rotational angular-momentum operator. The conical well V_{hin} which is divided into the regions I ($0 \leqslant \theta \leqslant \alpha$) and II ($\alpha < \theta \leqslant \pi$) is given by

$$V_{\text{hin}}(\theta) = \begin{cases} 0, & 0 \leqslant \theta \leqslant \alpha, \\ V_0, & \alpha < \theta \leqslant \pi, \end{cases} \tag{2}$$

where α is the hindrance angle and V_0 is the barrier height of the conical well.[17] Moreover, V_{ext} describes a dipolar molecule coupling with a static electric field

$$V_{\text{ext}} = -\omega \cos\theta, \tag{3}$$

with the field strength parameter $\omega = \mu\varepsilon$. Here, μ is the dipole moment of the molecule and ε is the electric field. The magnitude of the field strength parameter ω can be effectively modulated by the electric field.

To determine the heat capacity of adsorbed molecules, the standard procedure is to calculate the rotational-state energies. The whole system can be derived from the case without the electric field.[22–24] By solving the Schrödinger equation of the Hamiltonian $H_0 = B\mathbf{J}^2 + V_{\text{hin}}$, one obtains the eigenvalues

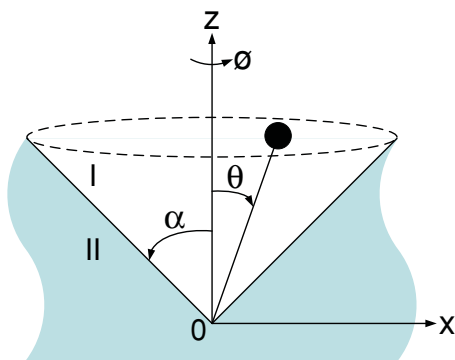$$\epsilon_{l,m} = \upsilon_{l,m}^I \left(\upsilon_{l,m}^I + 1 \right) B, \tag{4}$$

FIG. 1. (Color online) Schematic representation of a conical well with a hindrance angle α. The structure of the well is independent of azimuthal angle ϕ, and is further divided into the regions I ($0 \leqslant \theta \leqslant \alpha$) and II ($\alpha < \theta \leqslant \pi$), respectively. The filled circle denotes the molecular moment of inertia and θ is the angle of rotation with respect to the z axis.

where $\upsilon_{l,m}^{I}$ is a continuous positive number with the quantum number (l,m).[17] The (l,m) and $(l,-m)$ states are degenerate. After matching the boundary condition at the angle α, the value of $\upsilon_{l,m}^{I}$ is determined from the following equation

$$P_I\left(\upsilon_{l,m}^I,m,\zeta^*\right)P_{II}'\left(\upsilon_{l,m}^{II},m,\zeta^*\right)$$
$$-P_I'\left(\upsilon_{l,m}^I,m,\zeta^*\right)P_{II}\left(\upsilon_{l,m}^{II},m,\zeta^*\right)=0, \quad (5)$$

with $\upsilon_{l,m}^{II}(\upsilon_{l,m}^{II}+1)=\upsilon_{l,m}^{I}(\upsilon_{l,m}^{I}+1)-V_0/B$ and $P_{I(II)}'=dP_{I(II)}/d\zeta$ for $\zeta=\cos\theta$ and $\zeta^*=\cos\alpha$. The functions P_I and P_{II} are described as

$$P_I\left(\upsilon_{l,m}^I,m,\zeta\right)=(1-\zeta^2)^{|m|/2}F$$
$$\times\left(|m|-\upsilon_{l,m}^I,1+|m|+\upsilon_{l,m}^I,1+|m|;\frac{1-\zeta}{2}\right), \quad (6)$$

and

$$P_{II}\left(\upsilon_{l,m}^{II},m,\zeta\right)=(1-\zeta^2)^{|m|/2}F$$
$$\times\left(|m|-\upsilon_{l,m}^{II},1+|m|+\upsilon_{l,m}^{II},1+|m|;\frac{1+\zeta}{2}\right), \quad (7)$$

with F representing the hypergeometric function.[25] Correspondingly, the eigenfunctions read

$$\psi_{l,m}\left(\theta,\phi\right)=\begin{cases}C_{l,m}^I P_I\left(\upsilon_{l,m}^I,m,\zeta\right)\exp(im\phi), & \zeta^*\leqslant\zeta\leqslant 1,\\ C_{l,m}^{II}P_{II}\left(\upsilon_{l,m}^{II},m,\zeta\right)\exp(im\phi), & -1\leqslant\zeta<\zeta^*,\end{cases}$$
$$(8)$$

where $C_{l,m}^I$ and $C_{l,m}^{II}$ are the normalization constants.[17] From the basis of $\psi_{l,m}$, the wave function of the total Hamiltonian is given by $\Psi_{\sigma,m}(\theta,\phi)=\sum_{l,m}c_{l,m}\psi_{l,m}(\theta,\phi)$ for the (σ,m) energy state. By solving

$$H\Psi_{\sigma,m}=E_{\sigma,m}\Psi_{\sigma,m}, \quad (9)$$

one can numerically determine the energy $E_{\sigma,m}$ and wave function $\Psi_{\sigma,m}$ of the adsorbed molecule in the presence of the electric field.

From the energy spectrum, the thermodynamic properties are generated for adsorbed molecule system. The heat capacity of adsorbed molecules is given by

$$C_V=k_BT\frac{d^2}{dT^2}\left(T\ln Z\right), \quad (10)$$

where k_B is the Boltzmann constant, T is the temperature, and Z is the partition function denoted by

$$Z=\sum_{\sigma,m}\exp(-E_{\sigma,m}/k_BT). \quad (11)$$

To capture the main features of hindered rotation, we consider low temperature into the calculation. The energy scale of temperature is comparable to the rotational constant. Unless specified, calculations are performed for a barrier height of the conical well $V_0/B=50$ and a hindrance angle $\alpha=30°$.

III. RESULTS AND DISCUSSION

Figure 2 shows the low-lying rotational-state energies in the electric field. The behavior of energy spectrum strongly depends on the orientation of the field. As $\omega>0$, the spectrum shows negative shifts. The energies diminish with the electric field increasing. The result is similar to the free-rotor case.[5,26,27] In the case of $\omega<0$, however, the spectrum shows an interesting property because of the quantum confinement effect. The positive and negative energy shifts are obtained by varying the electric field. Specifically, the adjacent energy levels exhibit anticrossing phenomena due to the same quantum number m. For the lowest energy, one can discover an anticrossing behavior between the (0,0) and (1,0) energy levels at $\omega^*/B=-22.47$ (arrow). The energy gap between the two states is $\Delta^*/B=0.006$ shown in the inset.

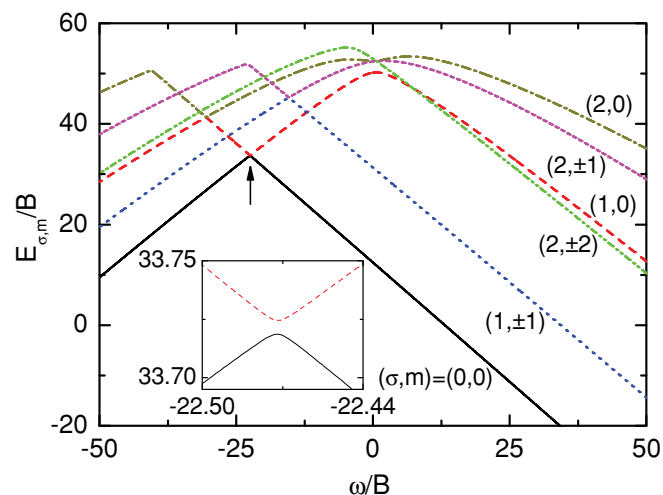To observe more clearly the confinement effect, the spatial distribution of wave function is analyzed in the well. The

FIG. 2. (Color online) Low-lying energy levels as a function of field strength parameter for $V_0/B=50$ and $\alpha=30°$. The arrow indicates an anticrossing between the (0,0) and (1,0) energy levels, as enlarged in the inset.
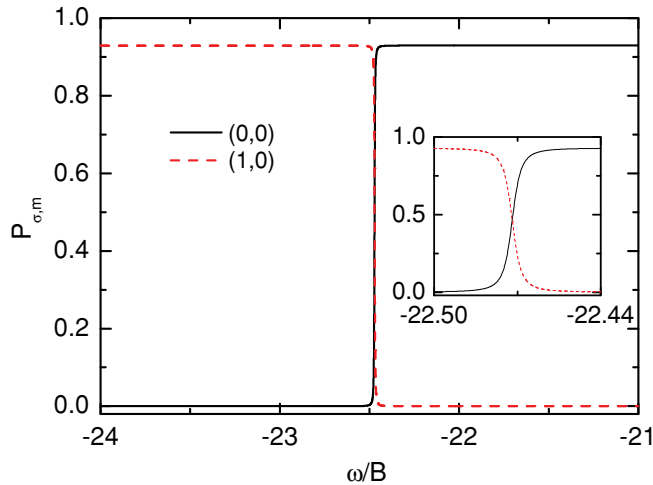
FIG. 3. (Color online) Probabilities of the (0,0) and (1,0) energy stats appearing inside the conical well. A drastic transformation in the probabilities is shown in the inset.
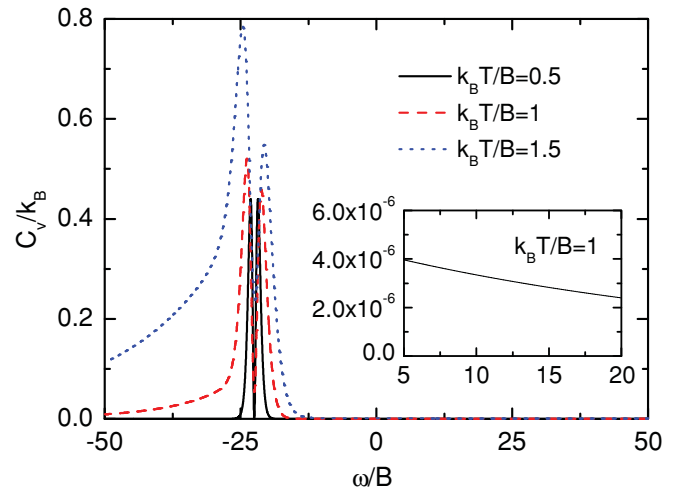

FIG. 4. (Color online) Heat capacity as a function of field strength parameter for different temperatures. The inset shows the heat capacity for $\omega > 0$ and $k_BT/B = 1$.

probability of the (σ,m) energy state appearing inside the conical well (region I) is given by

$$P_{\sigma,m} = \int_0^{2\pi} \int_0^{\alpha} |\Psi_{\sigma,m}(\theta,\phi)|^2 d\theta d\phi. \qquad (12)$$

In region II, the corresponding probability is thus $1 - P_{\sigma,m}$. The probabilities $P_{\sigma,m}$ for the (0,0) and (1,0) energy levels are plotted in Fig. 3. In general, the values smoothly vary with the electric field. Near the anticrossing area, the probability undergoes drastic transformation as shown in the inset. For $\omega > \omega^*$, the (0,0) state mostly appears inside the well (region I), while the (1,0) state spreads outside the well (region II). For instance, the ratio of $P_{0,0}$ to $P_{1,0}$ is around $174 : 1$ at $\omega/B = -22.45$. When the electric field increases, the rotor will be pushed to overcome the hindered potential. This phenomenon leads to an inversion in the probabilities of the two states in the case of $\omega < \omega^*$. However, if the barrier height approaches to infinity ($V_0 \to \infty$), the rotation of the molecule is only confined in region I.[16] Such transformed characteristics are suppressed in the infinite conical well.

Subsequently, we turn to discuss the thermodynamic property of adsorbed molecules in the electric field. Figure 4 illustrates the heat capacity for different temperatures. In the low-temperature region, the low-lying rotational energy states are contributed primarily to the heat capacity. For $\omega > 0$, the heat capacity is much small. The value of C_V/k_B is 3.3×10^{-6} at $\omega/B = 10$ and $k_BT/B = 1$ (inset). This value is generated due to large energy gaps between the states. On the contrary, the inverse electric field leads to a remarkable heat capacity. One can find two explicit peaks with modulating the electric field. As the temperature rises, both peaks shift and become asymmetric with each other. The ratio of the left to right peaks is $1.4 : 1$ at the temperature $k_BT/B = 1.5$. In particular, the heat capacity exhibits a dip between both peaks. The position of the dip is fixed with the temperatures. Such a feature corresponds to the position ($\omega = \omega^*$) at which the (0,0) and (1,0) states avoid crossing.

To examine the low-temperature behavior, we solely consider the (0,0) and (1,0) energy levels. The corresponding

partition is $Z = \exp(-E_{0,0}/k_BT) + \exp(-E_{1,0}/k_BT)$. From Eq. (10), the heat capacity is described as

$$C_V = k_B \left(\frac{\Delta}{2k_BT}\right)^2 \text{sech}^2 \left(\frac{\Delta}{2k_BT}\right), \qquad (13)$$

with the energy difference $\Delta = E_{1,0} - E_{0,0}$. The heat capacity based on the two-level model is plotted in Fig. 5 (red open circle). The approximation shows a symmetry-like behavior. Compared to the exact result based on Eq. (10) (solid line), the asymmetric effect on the peaks results from higher energy levels. It is clearly shown that the heat capacity drops at the anticrossing point, where $\Delta^* \ll k_BT$. We estimate the maximum of the heat capacity according to Eq. (13). The position of peak is determined by the equation

$$\tanh\left(\frac{\Delta}{2k_BT}\right) - \frac{2k_BT}{\Delta} = 0. \qquad (14)$$

One can find that the peak occurs at $\Delta \simeq 2.4k_BT$, corresponding to a Schottky anomaly. A similar feature has been manifested in different physical systems.[28,29] As obviously depicted in Figs. 2 and 5, the unique energy structure leads to two Schottky anomalies at $\omega/B = -21.12$ and -23.81, respectively. Although the same energy gaps result in the anomalies, the left and right peaks correspond to diverse distributions of the (0,0) and (1,0) states in the conical well, as shown in Fig. 3.

When the barrier height V_0 increases, the confinement of the well becomes stronger. The rotation of the molecule is greatly bounded inside the well so that the structure of rotational-state energies is modified. To resolve the effect, Fig. 6 shows the heat capacity for different values of V_0. A shifting behavior is observed with increasing the field strength. In particular, the dip of the heat capacity is not fixed and is linearly dependent on V_0, as obviously seen in the inset. The stronger electric field is applied to overcome the stronger confinement. One can expect that, if V_0 is infinite, the distinctive feature will disappear because of the anticrossing disappearance.

In addition to the barrier height, the hindrance angle is another structural parameter of the conical well. In Fig. 7
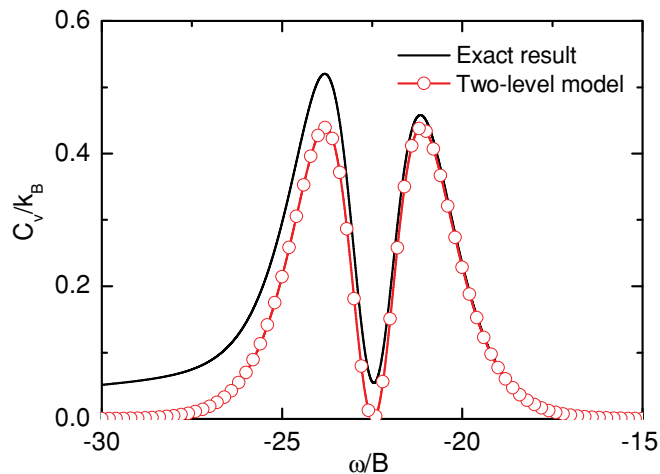
FIG. 5. (Color online) Heat capacity near the anticrossing between the (0,0) and (1,0) energy levels. The approximation based on the two-level model is compared with the exact result at the temperature $k_B T/B = 1$.

we plot the heat capacity for different hindrance angles. The two-peak behavior still exhibits at $\alpha = 60°$. As the angle increases, region II gets reduced gradually. The spatial confinement becomes weak so that the structure of the energy levels approximates to that of the free rotor. One can find a new peak around $\omega = 0$. In addition, the two adjacent peaks are reduced to the single one. This phenomenon can be understood by the fact that the energy gap between the (0,0) and (1,0) states is larger than the energy scale $k_B T$. Correspondingly, the anticrossing-related influence diminishes with the angle increasing. It is clearly shown that the associated peak is swept in the case of large angle ($\alpha = 160°$). One should note that the parameters α and V_0 can describe the realistic systems.[22,23] The magnitude of the parameters is estimated according to the results of the experiments.[15,30] It is the reason that the measured properties are closely related to the rotational states
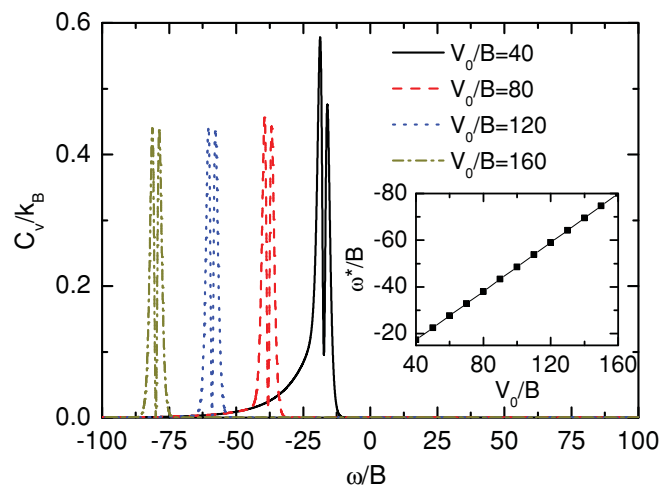

FIG. 6. (Color online) Heat capacity as a function of field strength parameter for different barrier heights. The inset shows the dependence of the specific parameter ω^* on the barrier height V_0. The temperature is $k_B T/B = 1$.
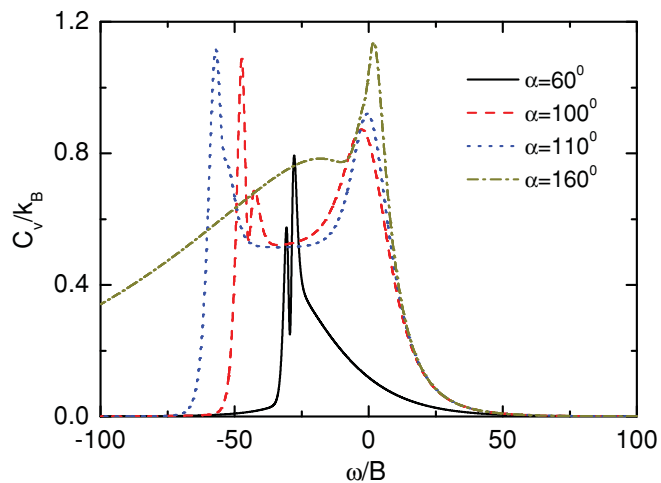

FIG. 7. (Color online) Heat capacity as a function of field strength parameter for different hindrance angles. The temperature is $k_B T/B = 1$.

of the adsorbed molecules. Consequently, one can extract the values of α and V_0 by fitting the calculated results to the measured data.

To provide more insight into the model, we analyze the wave functions of the ground and first excited states in detail. The wave function manifests the property of the rotational invariance [i.e., $\Psi_{\sigma,m}(\theta + 2n\pi, \phi) = \Psi_{\sigma,m}(\theta, \phi)$ with integer n]. The periodic situation is similar to the case of the Kronig-Penney model.[31,32] By employing the analogy accordingly, the conical well can be described as a periodic potential of polar angle θ. The potential within a period $0 \leqslant \theta \leqslant 2\pi$ is given by

$$V(\theta) = \begin{cases} -\omega \cos\theta, & 0 \leqslant \theta \leqslant \alpha, \\ V_0 - \omega \cos\theta, & \alpha < \theta \leqslant \pi + \alpha, \\ -\omega \cos\theta, & \pi + \alpha < \theta \leqslant 2\pi. \end{cases} \quad (15)$$

The electric field plays a critical role in altering the profile of the potential. For $\omega < \omega^*$, the potential for the region ($\alpha < \theta \leqslant \pi + \alpha$) is higher than that for the other two regions. As shown in Fig. 3, the ground state would localize in the regions ($0 \leqslant \theta \leqslant \alpha$) and ($\pi + \alpha < \theta \leqslant 2\pi$). On the contrary, the first excited state distributes in the region ($\alpha < \theta \leqslant \pi + \alpha$) due to the orthogonality of the wave functions. If ω is tuned to cross the point ω^*, however, the profile of the potential varies and exhibits a new local minimum in the region ($\alpha < \theta \leqslant \pi + \alpha$). This region becomes dominant over the others. To obtain a stable system, the wave functions of the states attempt to redistribute among the regions. Such redistributions of the wave functions change the tendencies of the energy levels so that the anticrossing feature occurs.

We briefly make some comparison with those used in related studies. For external dynamic influence, the adsorbed molecule is irradiated by a few-cycle laser field. The rotation of the molecule shows a periodic oscillation that can be characterized by orientation $\langle \cos\theta \rangle$. The variation of the orientation correlates with the rotational states.[7,33] The values of $\langle \cos\theta \rangle = 0$ and ± 1 correspond to random and perfect orientations, respectively. For the model, the features of the oscillation strongly depend on the parameters of the well.[24] For small α, the confining conical well causes the orientation

to show a large value. On the contrary, a large oscillatory amplitude of orientation is obtained in the case of large α. In the presence of the conical well, the positive orientation is not equivalent to the negative one. These results come from the confinement effect and differ from the case of free rotor.[24]

The features of heat capacity can provide useful information about the quantum systems.[34,35] For quantum-dot and magnetic systems, the structure of energy levels is tuned with the help of magnetic field. The heat capacity displays two peaks in the presence of crossing or anticrossing between the low-lying energy levels.[28,29] However, in the model exploited by this study, the electric field effectively controls the rotational properties of the adsorbed molecule. The heat capacity reflects the quantum effect of the hindered rotation. Similarly, a two-peak behavior exhibits in the heat capacity. The significant fact proves that the low-lying rotational levels repel with each other. Consequently, the heat capacity provides an approach to probe the fundamental energy structure of the hindered molecule.

The heat capacity of the adsorbed-molecule system may be measured by the calorimeter and related instruments. In principle, one prepares two different samples to determine the heat capacity. One sample is pure without molecular adsorption. The other sample corresponds to the situation that the molecules are adsorbed on the surface. From the measured data of two samples, the heat capacity of adsorbed molecules may be obtained by subtracting the contribution of the pure sample. Since the molecular vibrations are hardly excited at low temperature, their contribution to the heat capacity is negligible. Accordingly, the low-temperature heat capacity is mainly attributed to the rotational states of adsorbed molecules. The experiments have been performed to characterize the properties of molecular adsorbates on the graphites, such as carbon monoxide, oxygen and nitrogen.[36–39] Furthermore, the system of fullerene encapsulated hydrogen molecules is measured toward the direction of probing the rotational contribution.[40] Although the direct evidence of rotational heat capacity of adsorbed molecules is not obvious, the physical properties involved with the rotational states have been demonstrated by various experiments.[13–15,30] Specifically, some interesting features of the observed results can be reasonably captured by the theoretical works based on the conical well model.[22,23] Therefore, the heat capacity predicted by the conical well model is likely to be proved with the advance of measurement technology.

IV. CONCLUSION

The heat capacity of an adsorbed molecule system is studied in the electric field. The confinement effect and field-molecule interaction lead to rich and intensive structure in the energy spectrum. The anticrossings between the energy levels are observed via tuning the electric field. Moreover, the low-temperature heat capacity exhibits two peaks in the vicinity of the anticrossing point. The behavior of heat capacity is further exploited by varying the parameters of the system. The anticrossing-related feature is suppressed in the extreme situations.

*yyliao@nuk.edu.tw

[1] T. P. Rakitzis, A. J. van den Brom, and M. H. M. Janssen, Science **303**, 1852 (2004).

[2] O. Ghafur, A. Rouzée, A. Gijsbertsen, W. K. Siu, S. Stolte, and M. J. J. Vrakking, Nat. Phys. **5**, 289 (2009).

[3] D. DeMille, Phys. Rev. Lett. **88**, 067901 (2002).

[4] J. M. Rost, J. C. Griffin, B. Friedrich, and D. R. Herschbach, Phys. Rev. Lett. **68**, 1299 (1992).

[5] K. von Meyenn, Z. Phys. **231**, 154 (1970).

[6] B. Friedrich and D. Herschbach, Phys. Rev. Lett. **74**, 4623 (1995).

[7] M. Machholm and N. E. Henriksen, Phys. Rev. Lett. **87**, 193001 (2001).

[8] H. Stapelfeldt and T. Seideman, Rev. Mod. Phys. **75**, 543 (2003).

[9] E. Charron, P. Milman, A. Keller, and O. Atabek, Phys. Rev. A **75**, 033414 (2007).

[10] K. Mishima and K. Yamashita, J. Chem. Phys. **130**, 034108 (2009).

[11] W. Ho, J. Chem. Phys. **117**, 11033 (2002).

[12] K. Svensson and S. Andersson, Phys. Rev. Lett. **98**, 096105 (2007).

[13] L. Bengtsson, K. Svensson, M. Hassel, J. Bellman, M. Persson, and S. Andersson, Phys. Rev. B **61**, 16921 (2000).

[14] J. Z. Larese, T. Arnold, L. Frazier, R. J. Hinde, and A. J. Ramirez-Cuesta, Phys. Rev. Lett. **101**, 165302 (2008).

[15] I. Beauport, K. Al-Shamery, and H.-J. Freund, Chem. Phys. Lett. **256**, 641 (1996).

[16] J. W. Gadzuk, U. Landman, E. J. Kuster, C. L. Cleveland, and R. N. Barnett, Phys. Rev. Lett. **49**, 426 (1982).

[17] Y. T. Shih, D. S. Chuu, and W. N. Mei, Phys. Rev. B **51**, 14626 (1995).

[18] H. Shima and T. Nakayama, Phys. Rev. B **71**, 155210 (2005).

[19] A. G. M. Schmidt, J. Phys. A: Math. Theor. **42**, 245304 (2009).

[20] J. M. Brown and A. Carrington, *Rotational Spectroscopy of Diatomic Molecules* (Cambridge University Press, Cambridge, England, 2003).

[21] M. Iñarrea, J. P. Salas, R. González-Férez, and P. Schmelcher, Phys. Lett. A **374**, 457 (2010).

[22] Y. T. Shih, D. S. Chuu, and W. N. Mei, Phys. Rev. B **54**, 10938 (1996).

[23] Y. T. Shih, Y. Y. Liao, and D. S. Chuu, Phys. Rev. B **68**, 075402 (2003).

[24] Y. Y. Liao, Y. N. Chen, W. C. Chou, and D. S. Chuu, Phys. Rev. B **73**, 115421 (2006).

[25] *Handbook of Mathematical Functions with Formulas, Graphs and Mathematical Tables*, edited by M. Abramowitz and I. A. Stegun (Dover, New York, 1965).

[26] S. K. Sekatskii, Phys. Rev. A **75**, 052505 (2007).

[27] T. E. Wall, S. K. Tokunaga, E. A. Hinds, and M. R. Tarbutt, Phys. Rev. A **81**, 033414 (2010).

[28] J. H. Oh, K. J. Chang, G. Ihm, and S. J. Lee, Phys. Rev. B **50**, 15397 (1994).

[29] M. Affronte, A. Cornia, A. Lascialfari, F. Borsa, D. Gatteschi, J. Hinderer, M. Horvatić, A. G. M. Jansen, and M.-H. Julien, Phys. Rev. Lett. **88**, 167201 (2002).

[30] J. Xu, A. Barnes, R. Albridge, C. Ewig, N. Tolk, and L. D. Hulett Jr., Phys. Rev. B **48**, 8222 (1993).

[31] R. de, L. Kronig, and W. G. Penney, Proc. R. Soc. London, Ser. A **130**, 499 (1931).

[32] G. Bastard, Phys. Rev. B **24**, 5693 (1981).

[33] D. Sugny, A. Keller, O. Atabek, D. Daems, C. M. Dion, S. Guérin, and H. R. Jauslin, Phys. Rev. A **69**, 033402 (2004).

[34] N. T. T. Nguyen and F. M. Peeters, Phys. Rev. B **78**, 045321 (2008).

[35] T. Iwata and M. Watanabe, Phys. Rev. B **81**, 014105 (2010).

[36] A. Inaba, T. Shirakami, and H. Chihara, J. Chem. Thermodyn. **23**, 461 (1991).

[37] R. Marx and B. Christoffer, Phys. Rev. B **37**, 9518 (1988).

[38] M. H. W. Chan, A. D. Migone, K. D. Miner, and Z. R. Li, Phys. Rev. B **30**, 2681 (1984).

[39] H. Wiechert and S. A. Arlt, Phys. Rev. Lett. **71**, 2090 (1993).

[40] Y. Kohama, T. Rachi, J. Jing, Z. Li, J. Tang, R. Kumashiro, S. Izumisawa, H. Kawaji, T. Atake, H. Sawa, Y. Murata, K. Komatsu, and K. Tanigaki, Phys. Rev. Lett. **103**, 073001 (2009).